STEM CELLS AND DEVELOPMENT
Volume 22, Number 7, 2013

DOI: 10.1089/scd.2012.0555

Altered Fate of Tendon-Derived Stem Cells Isolated from a Failed Tendon-Healing Animal Model of Tendinopathy

Yun Feng Rui,[1,2,*] Pauline Po Yee Lui,[1–3,*] Yin Mei Wong,[1,2] Qi Tan,[1,2] and Kai Ming Chan[1,2]

We hypothesized that altered fate of tendon-derived stem cells (TDSCs) might contribute to chondro-ossification and failed healing in the collagenase-induced (CI) tendon injury model. This study aimed to compare the yield, proliferative capacity, immunophenotypes, senescence, and differentiation potential of TDSCs isolated from healthy (HT) and CI tendons. TDSCs were isolated from CI and healthy Sprague-Dawley rat patellar tendons. The yield, proliferative capacity, immunophenotypes, and senescence of TDSCs (CI) and TDSCs (HT) were compared by colony-forming unit assay, BrdU assay, flow cytometry, and β-galactosidase activity assay, respectively. Their osteogenic and chondrogenic differentiation potentials and mRNA expression of tendon-related markers were compared using standard assays. More TDSCs, which showed a lower proliferative potential and a higher cellular senescence were present in the CI patellar tendons compared to HT tendons. There was a higher alkaline phosphatase activity and mineralization in TDSCs (CI) in both basal and osteogenic media. More chondrocyte-like cells and higher proteoglycan deposition, Sox9 and collagen type II expression were observed in TDSCs (CI) pellets upon chondrogenic induction. There was a higher protein expression of Sox9, but a lower mRNA expression of *Col1a1*, *Scx*, and *Tnmd* in TDSCs (CI) in a basal medium. In conclusion, TDSCs (CI) showed altered fate, a higher cellular senescence, but a lower proliferative capacity compared to TDSCs (HT), which might contribute to pathological chondro-ossification and failed tendon healing in this animal model.

Introduction

Chronic tendinopathy is a tendon disorder characterized by pain, swelling and impaired performance that is extremely common in athletes and in the general population with repetitive strain injuries of tendons [1]. Given its pathogenesis is largely unknown, many current interventions are based on theoretical rationale and clinical experience rather than specific manipulation of underlying pathophysiological pathways.

Histologically, the tendinopathic tissue shows a failed healing status characterized by increase in cellularity, vascularity, proteoglycan deposition, particularly, the oversulfated form and collagen matrix degradation. Tissue metaplasia, including chondrocyte phenotypes (also called fibrocartilaginous metaplasia), fatty infiltration, and bony deposits are occasionally observed in some patients with tendinopathy [2,3]. The presence of calcification worsens the clinical manifestation of tendinopathy with an increase in the rupture rate [4], slower recovery times [5], and a higher frequency of postoperative complications [6].

We have shown loss of matrix organization, ectopic chondrogenesis, and ossification as well as activity-related tendon pain in a collagenase-induced (CI) failed tendon-healing rat model [7,8]. These histopathological changes were also reported in tendinopathy. There was also increased cellularity, glycosaminoglycan content, collagen fiber disorganization, and presence of chondrocyte-like cells in rat supraspinatus tendons after forced treadmill running [9]. We observed expression of Sox9 and collagen type II in healing tendon cells at week 2 before the expression of these markers in chondrocyte-like cells and ossified deposits, which appeared at week 4 and week 12 in the CI animal model, respectively [7]. Recent studies reported that tendons harbored tendon stem/progenitor cells and they could differentiate into chondrocytes and osteoblasts [10,11]. We called these cells tendon-derived stem cells (TDSCs) to indicate the tissue from which the cells were isolated. Since tenocytes were reported not to possess multilineage differentiation potential in a previous study [12], we hypothesized that TDSCs might show altered fate in differentiation from tenocytes to nontenocytes and this

[1]Department of Orthopaedics and Traumatology, Faculty of Medicine, The Chinese University of Hong Kong, Hong Kong SAR, China.
[2]The Hong Kong Jockey Club Sports Medicine and Health Sciences Centre, Faculty of Medicine, The Chinese University of Hong Kong, Hong Kong SAR, China.
[3]Program of Stem Cell and Regeneration, School of Biomedical Science, The Chinese University of Hong Kong, Hong Kong SAR, China.
*These two authors have contributed equally to this work.

might contribute to tissue metaplasia and failed tendon healing [13–16]. This study, therefore, aimed to compare the yield, proliferative capacity, immunophenotypes, cellular senescence and, in vitro differentiation potential of TDSCs isolated from healthy tendon (HT) and pathological tendon of the CI animal model.

Materials and Methods

CI tendon injury model

This study was approved by the Animal Research Ethics Committee of the authors' institution. Twelve male Sprague-Dawley rats, (6 weeks, weight 150–220 g) were used. The procedures have been well-established and the histopathological changes were highly reproducible [7]. After anesthesia with 2.5% pentobarbital (4.5 mg/kg body weight), hairs over the lower limb were shaved. The patellar tendon was located by positioning the knee at 90°. Twenty microliters (0.015 mg/μL in 0.9% saline, i.e., 0.3 mg) of bacterial collagenase I (Sigma-Aldrich, St Louis, MO) (CI group) or saline (HT group) was injected into both patellar tendons (i.e., both limbs were injected with saline or both limbs were injected with collagenase) of each rat intratendinously with a 30G needle (6 rats/group). Free cage activity was allowed after injection. At week 2 after injection, these 12 rats were sacrificed and the patellar tendons of both limbs of each rat were harvested and pooled together ($n = 6$/group) for the isolation of TDSCs (HT) or TDSCs (CI). Week 2 was chosen for the isolation of TDSCs (CI) because the direct effect of collagenase subsided and tendon healing with an increase in cell proliferation occurred, while no chondrocyte-like cells were observed at this time point [7].

Isolation and culture of rat TDSCs

The procedures for the isolation of TDSCs from rat patellar tendon have been established [17]. Briefly, the midsubstance of patellar tendons were excised from rats overdosed with 2.5% sodium phenobarbital. Care was taken that only the midsubstance of the patellar tendon tissue, but not the tissue at the bone–tendon junction, was collected. Peritendinous connective tissue was carefully removed and the samples were stored in sterile phosphate-buffered saline (PBS). The tissues were minced, digested with type I collagenase (3 mg/mL; Sigma-Aldrich), and passed through a 70-μm cell strainer (Becton Dickinson, Franklin Lakes, NJ) to yield a single-cell suspension. The released cells were washed in PBS and resuspended in a complete culture medium [low-glucose Dulbecco's Modified Eagle's Medium (LG-DMEM; Gibco), 10% fetal bovine serum, 100 U/mL penicillin, 100 μg/mL streptomycin, and 2 mM L-glutamine] (all from Invitrogen Corporation, Carlsbad, CA). The isolated nucleated cells were plated at an optimal low cell density (50 nucleated cells/cm^2) for the isolation of stem cells and cultured at 37°C, 5%CO_2 to form colonies. The optimal initial seeding density for TDSC isolation was determined using the colony-forming assay based on the criteria: (1) that the colony size was not affected by colony-to-colony contact inhibition; colonies that were less than 2 mm in diameter and faintly stained were ignored, and (2) that the greatest number of colonies per nucleated cells was obtained. At day 2 after initial plating, the cells were washed twice with PBS to remove the non-adherent cells. At day 7–10, they were trypsinized and mixed together as passage 0 (P0). TDSCs were subcultured when they reached 80%–90% confluence. TDSCs (HT) and TDSCs (CI) at early passages (P3 and P5) were used for all experiments [18]. TDSCs were confirmed by stem cell-related surface marker expression, colony forming unit assay, osteogenic, adipogenic, and chondrogenic differentiation assays as described previously before being used for the experiments in this study [11].

Study design

The colony-forming ability, proliferation, immunophenotypes, cellular senescence, and in vitro differentiation potential (osteogenic and chondrogenic, Sox9 expression, tendon-related marker expression) of TDSCs (CI) and TDSCs (HT) were compared.

Colony-forming unit assay

Colony-forming unit assay was done as described previously [11]. Tendon-derived nucleated cells (CI) and tendon-derived nucleated cells (HT), with each isolated from 6 different donor rats and in triplicate were used in this study. Tendon-derived nucleated cells (CI) and tendon-derived nucleated cells (HT) were plated at the optimal cell density at 1,000 nucleated cells (compared at 10^2, 10^3, 10^4, 10^5 per 20 cm^2 according to the criteria listed above, results not shown) in 20-cm^2 dishes each and cultured in the complete culture medium for 7–10 days to form colonies. The cells were stained with 0.5% crystal violet (Sigma, St Louis, MO) for counting the number of cell colonies. Colonies that were less than 2 mm in diameter and those that were faintly stained were ignored. The total tendon-derived nucleated cells isolated from bilateral patellar tendons in the CI group and the HT group were recorded. The total number of colonies per rat (bilateral patellar tendons) was calculated.

Cell proliferation assay

Cell proliferation assay was done as described previously [18]. TDSCs (HT) and TDSCs (CI) at P3 were plated at 5,000 cells/well in the complete culture medium in a 96-well plate and incubated at 37°C, 5% CO_2. At day 5, cell proliferation was assessed using the BrdU assay kit (Roche Applied Science, Indianapolis, IN) according to the manufacturer's instruction. Briefly, the cells were labeled with 10 μL BrdU for 3 h at 37°C. The labeling medium was then removed by inverting the microplate. The cells were then fixed with 100 μL FixDenat solution and incubated for 30 min at 37°C. The microplate was then taped to remove FixDenat, and then 100 μL peroxidase-conjugated anti-BrdU antibodies were added to each well and incubated with the cells for 90 min at room temperature. After washing with PBS, 100 μL of a substrate solution [3, 3, 5, 5-tetramethylbenzidine dissolved in 15% (v/v) dimethylsulfoxide] was added to each sample for 30 min at room temperature. The absorbance at 370–492 nm was measured and reported.

Fluorescence-activated cell sorting analysis

Both TDSCs (HT) and TDSCs (CI) at passage 3 were harvested by trypsinization, washed twice with PBS, pelleted by

centrifugation at 350 *g* for 5 min at room temperature, and resuspended in the staining buffer (Becton Dickson, Franklin Lakes, NJ) at 2×10^6/mL for 15 min at 4°C. One-hundred microliters cell suspension was incubated with primary antibodies against rat CD90 and CD44 conjugated with phycoerythrin (PE) (ab33694 and ab23396; both from Abcam, Cambridge, UK), CD31 conjugated with fluorescein isothiocyanate (FITC) (ab33858; Abcam), and CD34 conjugated with FITC (sc-7324; Santa Cruz Biotechnology, Santa Cruz, CA), CD73 (551123; Becton Dickinson, Franklin Lakes, NJ), CD11b (ab8879; Abcam), and CD45 (ab10558; Abcam), without conjugation for 15 min at 4°C. Unbound antibodies were washed away by adding an ice-cold staining buffer. The cell pellet was resuspended in the staining buffer containing anti-mouse IgG1 conjugated with PE (sc-3764; Santa Cruz Biotechnology) for CD11b and CD73, anti-rabbit IgG conjugated with FITC (sc-3839; Santa Cruz Biotechnology) for CD45 detection for at least 15 min at 4°C. The cells were washed with ice-cold PBS containing 2% BSA before analysis using the LSRFortessa flow cytometer (Becton Dickinson, San Jose, CA). PE- or FITC-conjugated isotype-matched mouse IgG1 (IC002P or IC002F, R&D systems, Inc., Minneapolis, MN), mouse IgG1 (MAB002; R&D systems, Inc.), and rabbit IgG (ISO-XXXX; Epitomics, Burlingame, CA) were used as isotype controls. Cells at 10^4 were counted for each sample. The percentage of cells with a positive signal was calculated using the WinMDI Version 2.9 program (The Scripps Research Institute, La Jolla, CA).

Senescence-associated β-galactosidase activity assay

We followed our well-established protocol as described previously [18]. Fifty micrograms of protein from TDSCs (HT) and TDSCs (CI) at P5 were used for the assessment of senescence-associated β-galactosidase activity using the mammalian β-galactosidase assay kit (Thermo scientific, Inc., Rockford, IL) according to the manufacturer's instruction. The absorbance at 405 nm was measured and reported.

Osteogenic differentiation assay

TDSCs (HT) and TDSCs (CI) at P3 were plated at 4×10^3 cells/cm^2 in a 24-well plate and cultured in the complete culture medium until the cells reached confluence. They were then incubated in the complete culture medium or the osteogenic medium, which was a complete culture medium supplemented with 1 nM dexamethasone, 50 mM ascorbic acid, and 20 mM β-glycerolphosphate (all from Sigma-Aldrich) at 37°C, 5% CO_2 as described previously [11]. At day 3, the alkaline phosphatase (ALP) activity of TDSCs was assessed by ALP cytochemical staining assay. At day 0, 7, 14, and 21, the mineralization of TDSCs was assessed by Alizarin red S staining.

ALP cytochemical staining assay. Cells were washed with PBS and fixed with 70% EtOH for 30 min at 4°C. The cells were then equilibrated twice with the ALP buffer (0.15 M NaCl, 0.1 M Tris-HCl pH 9.5, 1 mM $MgCl_2$, and 0.1% Tween-20) for 5 min each. The ALP substrate solution (0.5 mg nitroblue tetrazolium chloride and 0.25 mg 5-bromo-4-chloro-3'indolyphosphate p-toluidine salt (BCIP) in 1 mL ALP buffer) was added to the cells for 20 min at 37°C. The color reaction was stopped by washing the cells with distilled water and the positive stain was viewed under the microscope. Cells showing ALP activity appears deep blue. The higher the color intensity, the higher is the ALP activity.

Alizarin Red S staining assay. To evaluate the mineralized nodule formation in vitro, the cell/matrix layer was washed with the PBS, fixed with 70% ethanol for 10 min, and stained with 0.5% Alizarin red S (pH 4.1; Sigma, St. Louis, MO) for 30 min. To quantitate the amount of Alizarin red S bound to the mineralized nodules, the cells were rinsed with water, and extracted with 10% (w/v) cetylpyridinium chloride in 10 mM sodium phosphate, pH 7.0 for 15 min at room temperature. The dye concentration in the extract was determined at OD 562 nm in a 96-well plate.

Immunocytochemical staining

Immunocytochemical staining of Sox 9 in TDSCs (HT) and TDSCs (CI) was performed according to the procedures described earlier [11]. Five thousand TDSCs (HT) and TDSCs (CI) each at P3 were seeded on poly-L-lysine precoated 22×22 mm^2 glass coverslips at 37°C, 5% CO_2 overnight. The cells were then fixed in 4% paraformaldehyde, quenched with 10% H_2O_2 in methanol for 20 min, blocked with 5% normal goat serum, and incubated with rabbit polyclonal anti-rat Sox9 (1:30; sc-20095; Santa Cruz Biotechnology) for 30 min at room temperature. The primary antibody was replaced with a blocking solution in the negative controls. After washing with PBS, the cells were incubated with goat anti-rabbit horseradish peroxidase (HRP) (1:100; AP132P; Chemicon International, Temecula, CA) for 20 min at room temperature. Finally, 3, 3' diaminobenzidine tetrahydrochloride (DAKO, Glostrup, Denmark) was used to develop the color in the presence of H_2O_2. The cells were rinsed in distilled water, counterstained with Harris hematoxylin, dehydrated through graded alcohol, and mounted with p-xylene-bis-pyridinium bromide (DPX) (Sigma Aldrich). For good reproducibility and comparability, all incubation times and conditions were strictly controlled. The cells were examined under light microscopy (Leica DMRXA2, Leica Microsystems Wetzlar GmbH, Wetzlar, Germany).

Chondrogenic differentiation assay

A pellet culture system was used [11,18]. TDSCs (HT) and TDSCs (CI) at P3 were used. TDSCs (HT) and TDSCs (CI) at 8×10^5 were pelleted into a micromass by centrifugation at 450 *g* for 10 min in a 15-mL conical polypropylene tube and cultured in the complete culture medium or the chondrogenic medium, which contained the low-glucose Dulbecco's Modified Eagle's Medium (Gibco, Invitrogen corporation), supplemented with 10 ng/mL transforming growth factor-β3 (R&D), 500 ng/mL bone morphogenetic protein (BMP)-2 (R&D Systems, Inc.), 10^{-7} M dexamethasone, 50 μg/mL ascorbate-2-phosphate, 40 μg/mL proline, 100 μg/mL pyruvate (all from Sigma-Aldrich), and 1:100 diluted ITS + Premix (6.25 mg/mL insulin, 6.25 mg/mL transferrin, 6.25 mg/mL selenous acid, 1.25 mg/mL bovine serum albumin, 5.35 mg/mL linoleic acid) (Becton Dickinson, Franklin Lakes, NJ), at 37°C, 5% CO_2. At day 21, the pellets were fixed for hematoxylin and eosin (H&E), Safranin-O (SO)/fast green staining as well as immunohistochemical staining of Sox9 and collagen type II [18]. Semiquantitative image analysis of immunopositive signals of SO, Sox9, and collagen type II was done using the

Image-Pro Plus software (MediaCybernetics, Bethesda, MD) according to our well-established protocol [19].

Histological analysis of cell pellet. The cell pellets were fixed in 4% paraformaldehyde, dehydrated, and embedded in paraffin. Sections were cut at a thickness of 5 μm and were stained with H&E or SO/fast green after deparaffination and viewed using a LEICA Q500MC microscope (Leica Cambridge Ltd., Cambridge, UK). The mean integrated optical density (IOD) of SO in the histological sections were measured semiquantitatively using an image analysis method.

Immunohistochemical staining of cell pellet. Immunohistochemical staining was performed as previously described [18]. Briefly, paraffin-embedded sections were deparaffinized in xylene and dehydrated through graded alcohol. Endogenous peroxidase activity was quenched with 3% hydrogen peroxide for 20 min at room temperature. Antigen retrieval was then performed with 2 mg/mL protease (Calbiochem, Bie and Berntsen, Rødovre, Denmark) at 37°C for 30 min for collagen type II detection, and 1 mg/mL hyaluronidase at 37°C for 45 min followed by 10 nM warm citrate buffer at 65°C for 20 min for Sox 9 detection. Residual enzymatic activity was removed by washing the sections with PBS. After blocking the sections with 5% goat serum for 20 min at room temperature, the sections were incubated with mouse monoclonal antibodies against rat collagen type II (MS235-P; neomarkers-Biogen, Lab Vision, CA; 1:50 dilution with 5% goat serum in PBS containing 1% BSA) or rabbit monoclonal antibodies against rat Sox9 (sc-200955; Santa Cruz Biotechnology; 1:30 dilution with 5% goat serum in PBS containing 1% BSA) overnight at 4°C. The spatial localization of collagen type II and Sox9 was visualized by incubating the sections with goat anti-mouse IgG HRP-conjugated secondary antibodies (AP124P; 1:100; Chemicon International) for an hour at room temperature, followed by incubating the sections with 3,3';-diaminobenzidine tetrahydrochloride (DAKO) in the presence of H_2O_2. Afterward, the sections were rinsed, counterstained with hematoxylin, dehydrated with graded ethanol and xylene, and mounted with DPX. The primary antibody was replaced with the blocking solution in the sections that served as a negative control. Articular cartilage of femora condyle was used as a positive control for collagen type II and Sox9. The sections were examined under light microscopy (Leica DMRXA2, Leica Microsystems Wetzlar GmbH, Germany), and the immunopositive signal was semiquantified using an image analysis method.

Semiquantitative image analysis. The method is well-established in our laboratory [19]. Briefly, to analyze the positive signal, one photomicrograph from one section of each cell pellet was taken at 50× magnification under the same camera setting. We measured the positive signal using the Image-Pro Plus software (MediaCybernetics). First, the region of interest (ROI), which was the whole section of the cell pellet was selected manually. Segmentation of the image was then performed with the Select Colors command of the software. Three histograms on hue, saturation and intensity, respectively, would appear. The image was then segmented with a hue range of 1–33, a saturation range of 1–255, and an intensity range of 1–185 to select the light to dark brown color for immunohistochemical staining of collagen type II; a hue range of 1–33, a saturation range of 1–255, and an intensity range of 1–185 to select the light to dark brown color for immunohistochemical staining of Sox9; and a hue range of 1–33, a saturation range of 1–255, and an intensity range of 1–215 to select orange to red color for the SO staining of proteoglycan. The hue–saturation–intensity combinations were determined based on the samples showing the highest and the lowest expression to ensure that we covered the whole range of positive color that we would like to measure, while minimizing the interference from the background color of the image. To ensure reproducibility, the same hue–saturation–intensity combination was used for all samples. The IOD (in arbitrary unit) of the positive signal was then measured using the Count command of the software. The area of ROI was also measured. The IOD/μm^2 for each sample was reported. The assessor was blinded to the groups during image analysis.

Expression of tenogenic markers

TDSCs (HT) and TDSCs (CI) at P3 were seeded at 4×10^3 cells/cm^2 in a 24-well plate in the complete culture medium at 37°C, 5% CO_2. At day 3, the cells were harvested and the expression of tenogenic markers, including collagen type I (*Col1a1*), scleraxis (*Scx*), and tenomodulin (*Tnmd*) was examined by quantitative real-time reverse transcription–polymerase chain reaction (qRT-PCR) as described below.

Quantitative real-time reverse transcription–polymerase chain reaction

qRT-PCR was performed as previously described [18]. Cells were harvested and homogenized for RNA extraction with the Rneasy mini kit (Qiagen GmbH, Hilden, Germany). The mRNA was reverse transcribed to cDNA by the First-Strand cDNA kit (Promega, Madison, WI). 5 μL of total cDNA of each sample was amplified in the final volume of 25 μL of reaction mixture containing Platinum® SYBR® Green qPCR SuperMix-UDG ready-to-use reaction cocktail and specific primers for collagen type I (*Col1a1*), scleraxis (*Scx*), tenomodulin (*Tnmd*), or β-*actin* using the ABI StepOne Plus system (all from Applied Biosystems, Foster City, CA) (Table 1). Cycling conditions were denaturation at 95°C for 10 min, 45 cycles at 95°C for 20 s, optimal annealing temperature (Table 1) for 30 s, 72°C for 30 s, and finally at 60°C–95°C with a heating rate of 0.1°C/s. The expression of the target gene was normalized to that of the β-*actin* gene. Relative gene expression was calculated using the $2^{-\Delta CT}$ formula.

Data analysis

The mean IOD/μm^2 of different chondrogenic markers and the mRNA expression of tendon-related markers in the TDSCs (CI) and TDSCs (HT) groups were presented in boxplots. Comparison of 2 independent groups was done using the Mann–Whitney U test, while comparison of more than 2 independent groups was done using the Kruskal–Wallis test followed by post hoc pairwise comparison using the Mann–Whitney U test. All the data analysis was done using SPSS analysis software (SPSS, Inc., Chicago, IL; version 16.0). $P \leq 0.05$ was regarded as statistically significant.

Result

Stem cell characteristics of TDSCs (HT) and TDSCs (CI)

The nucleated cells isolated from healthy patellar tendons and CI pathological tendons at week 2 were stem cells as

Table 1. Primer Sequences and Condition for Quantitative Real-Time Reverse Transcription–Polymerase Chain Reaction

Gene	Primer nucleotide sequence	Product size (bp)	Annealing temperature (°C)	Accession no.
β-actin	5′-ATC GTG GGC CGC CCT AGG CA-3′ (forward) 5′-TGG CCT TAG GGT TCA GAG GGG-3′ (reverse)	243	52	NM_031144
Col1a1	5′- CATCGGTGGTACTAAC-3′ (forward) 5′- CTGGATCATATTGCACA-3′ (reverse)	238	55	NM_053356.1
Tnmd	5′-GTGGTCCCACAAGTGAAGGT-3′ (forward) 5′-GTCTTCCTCGCTTGCTTGTC-3′ (reverse)	60	52	NM_022290.1
Scx	5′-AACACGGCCTTCACTGCGCTG-3′ (forward) 5′-CAGTAGCACGTTGCCCAGGTG-3′ (reverse)	102	58	NM_001130508.1

indicated by their abilities to form colonies (Fig. 1b, b′). The cells in the colonies appeared less clustered in the CI group compared to those in the HT group (Fig. 1c, c′). The isolated cells from both groups showed multilineage differentiation potential as indicated by their abilities to form calcium nodules (Fig. 1d, d′), lipid droplets (Fig. 1e, e′), and chondrocyte pellets (Fig. 1f, f′) upon osteogenic, adipogenic, and chondrogenic induction, respectively.

Yield, proliferative potential, immunophenotypes, and cellular senescence of TDSCs

We counted the total number of colonies that were isolated from the patellar tendons of each rat at the optimal seeding density (50 nucleated cells/cm^2). There were more TDSCs colonies in the CI group compared to those in the HT group ($P = 0.050$) (Fig. 2a). TDSCs (CI) proliferated slower compared to TDSCs (HT) ($P = 0.009$) (Fig. 2b). TDSCs (HT) and TDSCs (CI) were both positive for mesenchymal stem cell markers, including CD90, CD44, and CD73, but negative for the endothelial cell marker, CD31, and hematopoietic lineage markers, including CD34, CD45, and CD11b (Fig. 2c, d). The surface expression of CD73 and CD44 was greatly and slightly reduced in TDSCs (CI) compared to TDSCs (HT) (Fig. 2c, d). TDSCs (CI) also showed significantly higher cellular senescence compared to TDSCs (HT) ($P = 0.025$) (Fig. 2e).

Osteogenic differentiation potential

There was higher ALP activity in the TDSCs (CI) group compared to that in the TDSCs (HT) group both in basal and osteogenic media at 3 days as indicated by the ALP cytochemical staining assay (Fig. 3a). Similarly, more alizarin red S-positive calcium nodules were observed in TDSCs (CI) compared to those in TDSCs (HT) both in basal and osteogenic media at day 7, 14, and 21 (Fig. 3b). Quantification of the intensity of calcium-bound alizarin red S signal showed that there was a significant higher signal intensity in TDSCs (CI) compared to that in TDSCs (HT) both in basal and osteogenic media at day 7, 14, and 21 (both overall $P < 0.001$, respectively; all post hoc $P = 0.004$) (Fig. 3c, d).

Chondrogenic differentiation potential

Most of the TDSCs in the CI group expressed Sox9, while only a few TDSCs in the HT group expressed this chondrogenic marker in the basal medium (Fig. 4a). We next tested the chondrogenic differentiation potential of TDSCs (HT) and TDSCs (CI) in the chondrogenic medium in a 3D pellet culture system (Fig. 4b). Our results showed that both TDSCs (HT) and TDSCs (CI) formed pellets at day 21, but more chondrocyte-like cells were observed in the TDSCs (CI) pellets compared to those in the TDSCs (HT) pellets (Fig. 4b

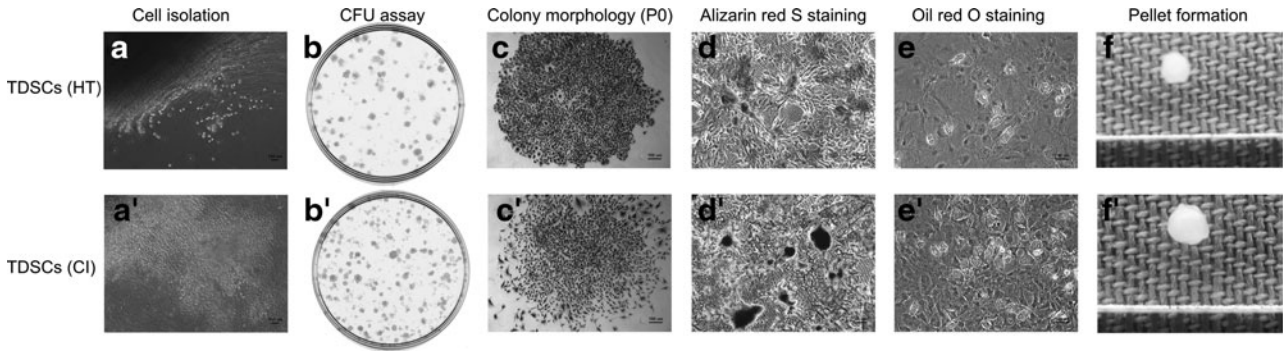

FIG. 1. Isolation and characterization of tendon-derived stem cells (TDSCs) (HT) **(a–f)** and TDSCs [collagenase-induced (CI)] **(a′–f′)** photomicrographs showing released tendon-derived nucleated cells from rat patellar tendons after collagenase type I digestion **(a, a′)**; clonogenicity of tendon-derived nucleated cells as indicated by colony-forming unit (CFU) assay **(b, b′)**; morphology of tendon-derived cell colonies formed at P0 **(c, c′)**; calcium nodules as detected by Alizarin red S staining of TDSCs after osteogenic induction **(d, d′)**; lipid droplets as indicated by Oil red O staining of TDSCs after adipogenic induction **(e, e′)**; pellet formation of TDSCs after chondrogenic induction **(f, f′)**. Scale bar: 100 μm **(c–e, c′–e′)**.

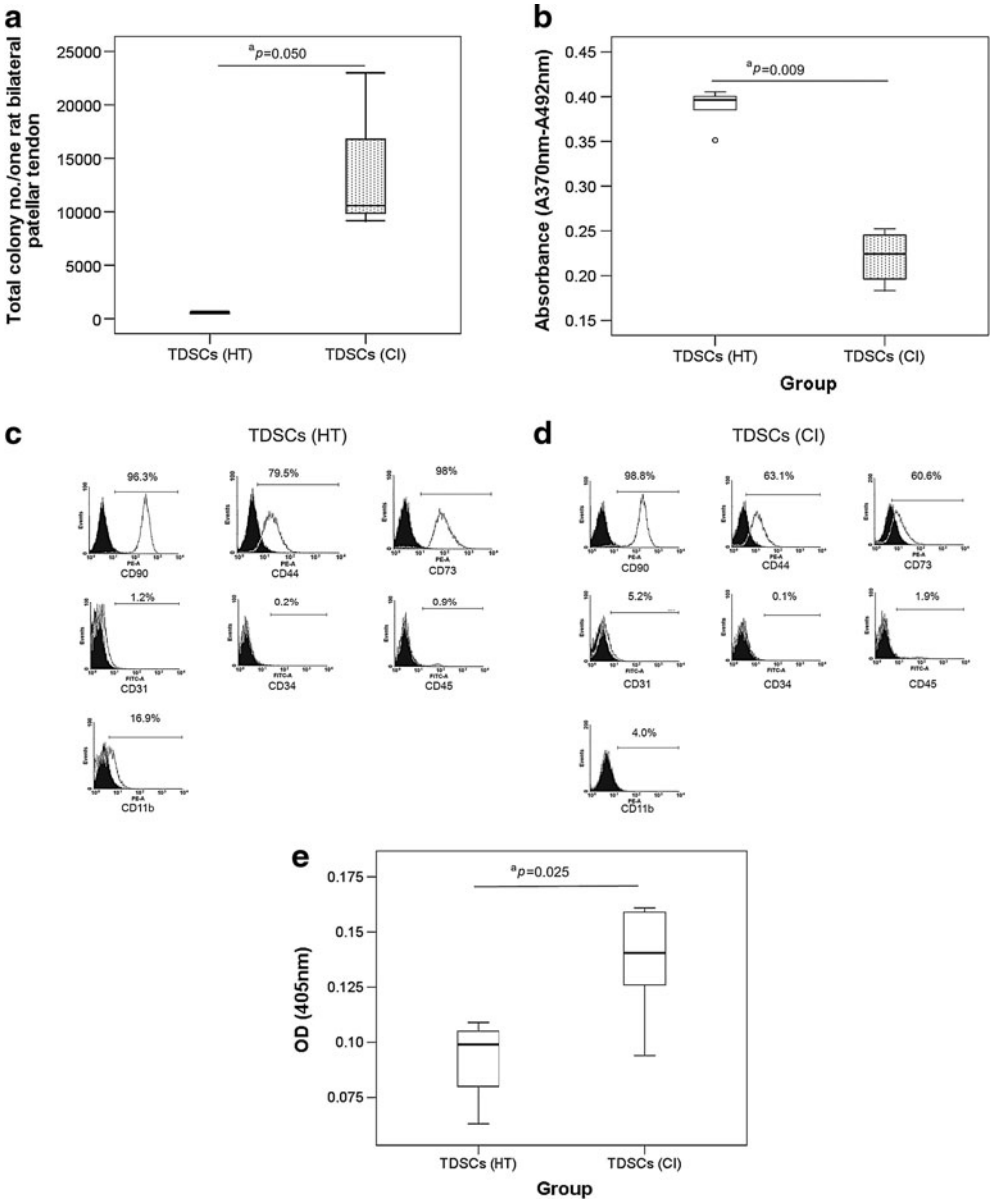

FIG. 2. **(a)** Box plot showing the yield of colonies in healthy patellar tendon and CI injured patellar tendon as assessed by colony-forming assay. $n=6$/group; $^aP\leq0.05$ **(b)** Box plot showing the proliferative capacity of TDSCs (CI) and TDSCs (healthy tendon [HT]) in vitro as measured by BrdU assay. "o" represented outliner in the study; $n=5$/group; $^aP\leq0.05$ **(c, d)** Histograms showing the surface expression of mesenchymal stem cell markers (CD90, CD44, and CD73), endothelial stem cell marker (CD31), and hematopoietic lineage markers (CD34, CD45, and CD11b) on TDSCs (HT) and TDSCs (CI). $n=1$/group; **(e)** Box plot showing the senescence-associated β-galactosidase activity in TDSCs (HT) and TDSCs (CI). $n=6$/group; $^aP\leq0.05$.

H&E staining). There was significantly higher proteoglycan deposition as indicted by SO staining ($P=0.021$), Sox9 expression ($P=0.021$), and collagen type II expression ($P=0.021$) in TDSCs (CI) pellets compared to that in TDSCs (HT) pellets (Fig. 4b).

Expression of tenogenic markers

We compared the tenogenic activity of TDSCs (HT) and TDSCs (CI) by measuring the mRNA expression of tendon-related markers. There was a significantly lower mRNA expression of *Col1a1* ($P=0.004$) (Fig. 5a), *Scx* ($P=0.004$) (Fig. 5b), and *Tnmd* ($P=0.006$) (Fig. 5c) in TDSCs (CI) compared to that in TDSCs (HT) in the basal medium.

Discussion

Our result showed that TDSCs (CI) showed a lower proliferative potential and a higher cellular senescence compared to TDSCs (HT). We also observed a higher osteogenic and chondrogenic differentiation potential of TDSCs (CI) in basal and induction media, but a lower tenogenic activity in the basal medium. Our results were consistent with the hypothesis of altered fate of TDSCs to nontenocytes and might explain the

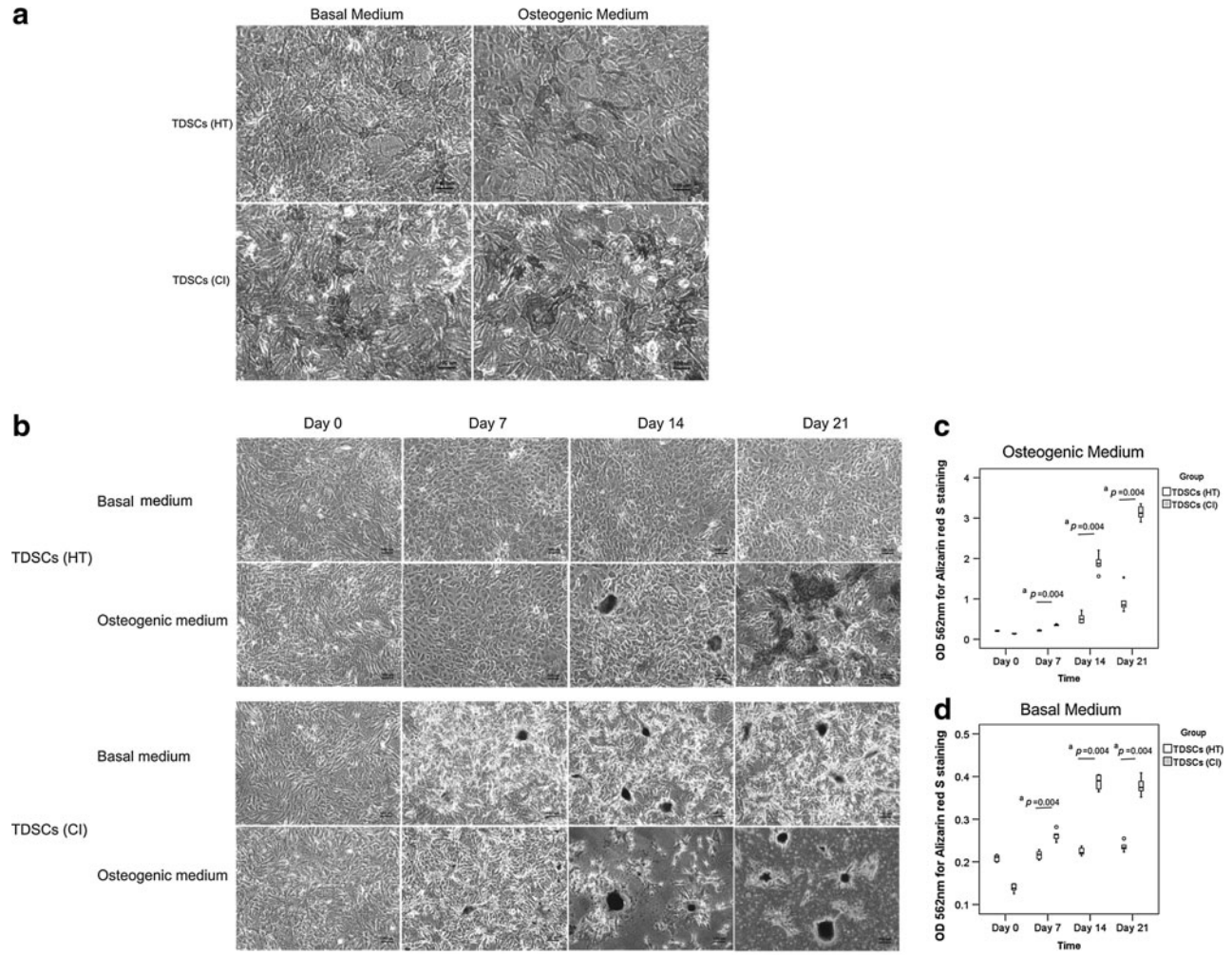

FIG. 3. **(a)** Photomicrographs showing alkaline phosphatase activity in TDSCs (HT) and TDSCs (CI) in both basal culture medium and osteogenic medium at day 3. $n=3$/group; Scale bar: 100 μm; basal culture medium: complete culture medium. **(b)** Photomicrographs showing Alizarin red S staining of calcium nodules formed in TDSCs (HT) and TDSCs (CI) in both basal medium and osteogenic medium at day 0, day 7, day 14, and day 21. $n=6$/group; Scale bar: 100 μm; basal culture medium: complete culture medium. **(c, d)** showed the quantitative analysis of the amount of Alizarin red S bound to the calcium nodules in osteogenic medium and basal medium, respectively. "o" and "*" represented outliner and extreme value, respectively, in the study. $n=6$/group; $^{a}P \leq 0.05$ in post hoc comparison.

formation of ectopic chondro-ossification in our CI animal model. The reduced ability of TDSCs to differentiate into tenocytes, coupled with their reduced proliferation and increased senescence might reduce the pool of TDSCs for tendon repair after tendon injury and might contribute to failed tendon healing in this animal model. The higher yield of TDSCs (CI) compared to TDSCs (HT) might be an attempt of the cells to compensate for the decrease in proliferative and tenogenic differential potential as well as an increased cellular senescence after CI tendon injury. In fact, we also observed higher adipogenic differentiation of TDSCs (CI) compared to TDSCs (HI) upon adipogenic induction as shown by Oil red O staining (Fig. 1e, e'). However, we did not quantify the amount of bound dye.

The results in this study provided some insights into the mechanism of tissue metaplasia and failed healing in tendinopathy. Supportive evidences for nontenogenic differentiation of TDSCs in the pathogenesis of tendinopathy included upregulation of cartilage-associated genes and downregulation of tendon-associated genes in rat supraspinatous tendon [15] and in horse superficial digital flexor tendon [16] after overuse injury. The development of fracture nonunion was suggested to link to the reduced capacity of the tissue-specific stem cells to undergo osteogenesis and increased cellular senescence [20]. Our results in the failed healing CI animal model in this study provided some support that tissue metaplasia and failed healing in tendinopathy might occur via altered fate of stem cells in tendon after tendon injury. Recently, Bi et al. [10] reported that tendon stem/progenitor cells (TSPCs) isolated from the biglycan and fibromodulin double knockout mouse model with ectopic bone and deranged collagen fibers in the patellar tendon showed higher clonogenicity and proliferation. TSPCs isolated from this double knockout animal model also expressed collagen type II and aggrecan, which were absent in wild-type TSPCs [10]. The protein expression of collagen type I and mRNA expression of *Scx* in TSPCs isolated from the double knockouts decreased compared to wild-type cells [10]. Moreover, TSPCs isolated from the double knockout animals formed bone in

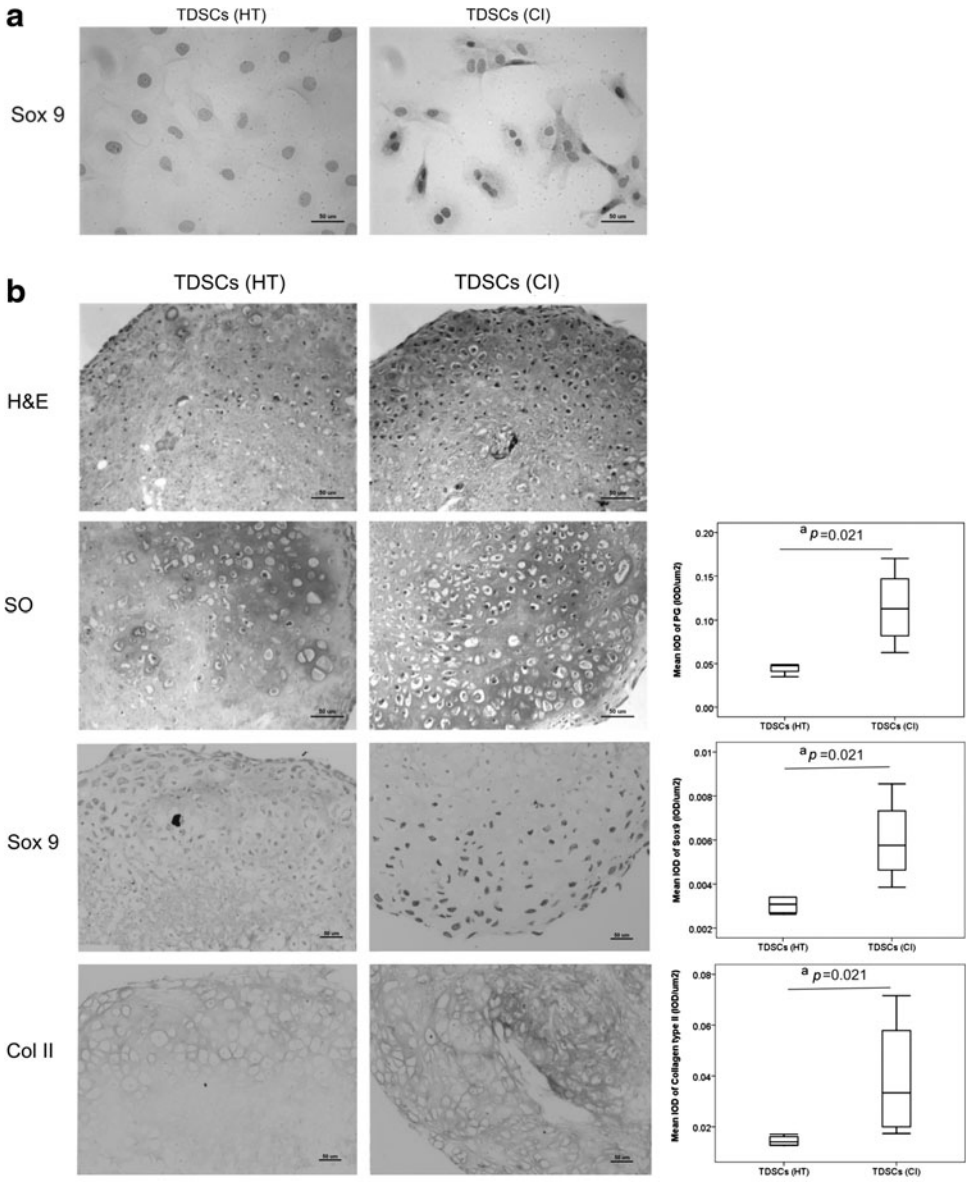

FIG. 4. (a) Photomicrographs showing the expression of Sox9 in TDSCs (HT) and TDSCs (CI). $n=3$/group; Scale bar: 50 μm. **(b)** Photomicrographs showing the cell morphology with hematoxylin and eosin (H&E) staining, proteoglycan accumulation with Safranin-O (SO) staining, Sox9 and collagen type II expression in cell pellets formed by TDSCs (HT) and TDSCs (CI) after culturing the cells in chondrogenic medium for 21 days. Box plots next to the photomicrographs are semi-quantitative image analysis of the positive signals of SO staining, Sox9 and collagen type II, respectively. All $n=4$/group; Scale bar: 50 μm; $^{a}P \leq 0.05$.

addition to tendon-like tissue in vivo, whereas wild-type TDSCs only formed tendon-like tissue [10]. Of note was that the animal model used by Bi et al. [10] was a transgenic animal model, while the animal model that we used in this study was biologically induced after birth.

For the factors that might possibly lead to the altered fate of TDSCs after collagenase injection, we hypothesized that the ectopic expression of BMP-2 and the change in extracellular matrix composition might alter the fate of TDSCs and contributed to tissue metaplasia and failed healing in the CI animal model. This speculation was supported by the change in the extracellular matrix composition, with a sustained increase in the type III to type I collagen ratio and proteoglycan expression, in the CI animal model [21]. There was also ectopic

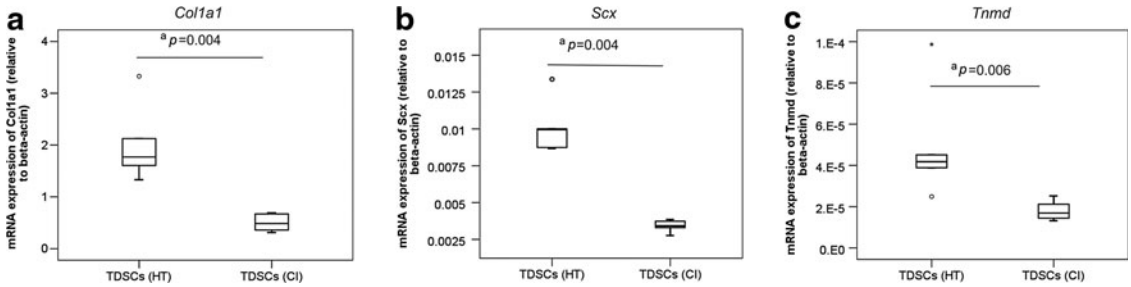

FIG. 5. Box plots showing the mRNA expression of **(a)** *Col1a1*, **(b)** *Scx*, and **(c)** *Tnmd* in TDSCs (HT) and TDSCs (CI). "o" and "*" represented outliner and extreme value, respectively, in the study. $n=6$/group; $^{a}P \leq 0.05$.

expression of BMP-2, BMP-4, and BMP-7 in the CI animal model [19] and clinical samples of patellar tendinopathy [22]. The increased deposition of proteoglycan and sulfate glycoaminoglycans was the characteristic extracellular matrix changes in tendinopathy [23,24]. Ectopic overexpression of BMPs was also observed in the subacromial bursa of patients with chronic degeneration of the rotator cuff [25]. We reported that cyclic tensile loading increased the mRNA and protein expression of BMP-2 in TDSCs in vitro [17]. In a separate study, BMP-2 also promoted the nontenocyte differentiation, increased the glycoaminoglycan deposition, and increased the mRNA expression of aggrecan in TDSCs in vitro [26]. Further study is required to confirm our speculation.

Our results showed that there was a large and slight reduction of surface expression of CD73 and CD44, respectively, in TDSCs (CI) compared to TDSCs (HT). CD73 was reported to function in cell–cell adhesion [27]. A previous study showed that the migration of mesenchymal stromal cells (MSCs) was controlled by the surface expression of CD73/CD29, which in turn was regulated by compressive mechanical loading of the cells [28]. Specific inhibition of CD73/CD29 inhibited MSCs migration after compressive mechanical loading in vitro [28]. The knockdown of CD73 was also reported to increase migration and collagen type I mRNA expression in a hepatic stellate cell line [29]. The decrease in the expression of CD73/CD29 was suggested as a mechanism for trapping MSCs in the injury site to fulfill their regenerative functions [28]. Whether the decrease in surface expression of CD73 in TDSCs (CI) was associated with reduced migration ability of these cells needs further research. The reduced mRNA expression of CD73 was also reported to positively correlate with the reduced proliferation and differentiation efficiency of human MSCs during passaging in vitro [30]. Hence, the reduction in the surface expression of CD73 might also be explained by the committed differentiation of TDSCs (CI) to the chondrogenic and osteogenic lineages. CD44 is a cell-surface glycoprotein, which participates in many cellular processes, which includes cell growth, survival, differentiation, and motility [31]. It is a receptor for hyaluronic acid and can also interact with other ligands, such as osteopontin, collagens, growth factors, and matrix metalloproteinases as well as function as a coreceptor to mediate the signaling of receptor tyrosine kinases [31]. Previous study showed that the expression of CD44 was important for the migration of mesenchymal stem cells [32]. Knockdown of CD44 was reported to promote the differentiation of cancer stem cells [33]. Hence, the slight reduction of surface expression of CD44 in TDSCs (CI) might also be related to the increased commitment of TDSCs (CI) toward the differentiated lineages.

One limitation of this study was that the source of stem cells contributing to altered functions could be endogenous or exogenous as there was no specific marker for TDSCs. This is also the case for other mesenchymal stem/progenitor cells, which were isolated by selection and enrichment methods. The composition of TDSCs might change depending on the physiological or pathological status of the animal or individual. However, this did not object our conclusion that stem cells isolated from tendon tissues (defined as TDSCs, similar terminology is also used to refer to the tissue-specific stem cells isolated from other tissues.) of the CI animal model showed a higher chondro-osteogenic, but a lower tenogenic differentiation potential and might contribute to tissue metaplasia and failed healing in this CI animal model. A similar mechanism might contribute to tissue metaplasia and failed tendon healing in tendinopathy. Further study to identify the subpopulation of TDSCs that showed altered differentiation potential is essential.

Conclusions

In conclusion, TDSCs (CI) showed altered fate with a higher osteogenic and chondrogenic differentiation potential, but a lower tenogenic differentiation capacity, a lower proliferative capacity, but a higher senescence and colony-forming ability compared to TDSCs (HT). These might contribute to the pathological chondro-ossification and failed tendon healing in this animal model. Results from this study provided insights into the mechanisms of tissue metaplasia and failed healing of tendinopathy.

Acknowledgments

This project is supported by equipment/resources donated by the Hong Kong Jockey Club Charities Trust and the CUHK Direct Grant (2009.1.043).

Prior conference presentation of part of the submitted material:

1. Lui PPY, YF Rui, YM Wong, Q Tan and KM Chan. Altered fate of tendon-derived stem cells (TDSCs) in ossified failed tendon healing. *In Proceedings of* The International Symposium on Ligaments & Tendons (ISL&T)-XII, 3rd Feb, 2012, Hilton Financial District, San Francisco, California, USA, poster presentation.
2. Rui YF, PPY Lui, YM Wong, LS Chan, YW Lee, M Ni, Q Tan, YW Lee and KM Chan. Impaired differentiation and proliferation of tendon-derived stem cells (TDSCs) isolated from collagenase-induced tendon injury model–A potential mechanism for the chondro-ossification and failed healing of tendinopathy. *In Proceedings of* 57th Annual Meeting of the Orthopaedic Research Society, 13th–16th Jan, 2011, Long Beach, California, USA, poster presentation.

Author Disclosure Statement

No competing financial interests exist.

References

1. Paavola M, P Kannus, TA Jarvinen, K Khan, L Jozsa and M Jarvinen. (2002). Achiles tendinopathy. J Bone Joint Surg Am 84-A:2062–2076.
2. de Mos M, W Koevoet, HTM ven Schie, N Lops, H Jahr, JAN Verhaar and GJVM van Osch. (2009). In vitro model to study chondrogenic differentiation in tendinopathy. Am J Sports Med 37:1214–1222.
3. Kannus P and L Jozsa. (1991). Histopathological changes preceding spontaneous rupture of a tendon. A controlled study of 891 patients. J Bone Joint Surg Am 73:1507–1525.
4. Jim YF, HC Hsu, CY Chang, JJ Wu and T Chang. (1993). Coexistence of calcific tendinitis and rotator cuff tear: an arthrographic study. Skeletal Radiol 22:183–185.
5. Hashimoto T, K Nobuhara and T Hamada. (2003). Pathologic evidence of degeneration as a primary cause of rotator cuff tear. Clin Orthop Relat Res 415:111–120.

6. Aina R, E Cardinal, NJ Bureau, B Aubin and P Brassard. (2001). Calcific shoulder tendinitis: treatment with modified US-guided fine-needle technique. Radiology 221:455–461.
7. Lui PPY, SC Fu, LS Chan, LK Hung and KM Chan. (2009). Chondrocyte phenotype and ectopic ossification in collagenase-induced tendon degeneration. J Histochem Cytochem 57: 91–100.
8. Lui PPY, LS Chan, SC Fu and KM Chan. (2010). Expression of sensory neuropeptides in tendon is associated with failed healing and activity-related tendon pain in collagenase-induced tendon injury. Am J Sports Med 38:757–764.
9. Scott A, JL Cook, DA Hart, DC Walker, V Duronio and KM Khan. (2007). Tenocyte responses to mechanical loading in vivo: a role for local insulin-like growth factor 1 signaling in early tendinosis in rats. Arthritis Rheum 56:871–881.
10. Bi Y, D Ehirchiou, TM Kilts, TM Kilts, CA Inkson, MC Embree, W Sonoyama, L Li, AI Leet, et al. (2007). Identification of tendon stem/progenitor cells and the role of the extracellular matrix in their niche. Nat Med 13:1219–1227.
11. Rui YF, PPY Lui, G Li, SC Fu, YW Lee and KM Chan. (2010). Isolation and characterization of multi-potent rat tendon-derived stem cells. Tissue Eng Part A 16:1549–1558.
12. Zhang J and JH Wang. (2010). Characterization of differential properties of rabbit tendon stem cells and tenocytes. BMC Musculoskelet Disord 11:10.
13. Rui YF, PP Lui, LS Chan, KM Chan, SC Fu and G Li. (2011). Does erroneous differentiation of tendon-derived stem cells contribute to the pathogenesis of calcifying tendinopathy? Chin Med J (Engl) 124:606–610.
14. Lui PP and KM Chan. (2011). Tendon-Derived Stem Cells (TDSCs): From basic science to potential roles in tendon pathology and tissue engineering applications. Stem Cell Rev 7:883–897.
15. Archambault JM, SA Jelinsky, SP Lake, AA Hill, DL Glaser and LJ Soslowsky. (2007). Rat supraspinatus tendon expresses cartilage markers with overuse. J Orthop Res 25:617–624.
16. Clegg PD, S Strassburg and RK Smith. (2007). Cell phenotypic variation in normal and damaged tendons. Int J Exp Patho 88:227–235.
17. Rui YF, PP Lui, M Ni, LS Chan, YW Lee and KM Chan. (2011). Mechanical loading increased BMP-2 expression which promoted osteogenic differentiation of tendon-derived stem cells. J Orthop Res 29:390–396.
18. Tan Q, PP Lui and YF Rui. (2012). Effect of in vitro passaging on the stem cell-related properties of tendon-derived stem cells–Implications in tissue engineering. Stem Cells Dev 21:790–800.
19. Yee Lui PP, YM Wong, YF Rui, YW Lee, LS Chan and KM Chan. (2011). Expression of chondro-osteogenic BMPs in ossified failed tendon healing model of tendinopathy. J Orthop Res 29:816–821.
20. Bajada S, MJ Marshall, KT Wright, JB Richardson and WEB Johnson. (2009). Decreased osteogenesis, increased cell senescence and elevated Dickkopf-1 secretion in human fracture non union stromal cells. Bone 45:726–735.
21. Lui PPY, LS Chan, YW Lee, SC Fu and KM Chan. (2010). Sustained expression of proteoglycans and collagen type III/Type I ratio in a calcified tendinopathy model. Rheumatology (Oxford) 49:231–239.
22. Rui YF, PP Lui, CG Rolf, YM Wong, YW Lee and KM Chan. (2012). Expression of chondro-osteogenic BMPs in clinical samples of patellar tendinopathy. Knee Surg Sports Traumatol Arthrosc 20:1409–1417.
23. Corps AN, AHN Robinson, T Movin, ML Costa, BL Hazleman and GP Riley. (2006). Increased expression of aggrecan and biglycan mRNA in Achilles tendinopathy. Rheumatology 45:291–294.
24. Parkinson J, T Samiric, MZ Ilic, J Cook, JA Feller and CJ Handley. (2010). Change in proteoglycan metabolism is a characteristic of human patellar tendinopathy. Arthritis Rheum 62:3028–3035.
25. Neuwirth J, RAE Fuhrmann, A Veit, M Aurich, I Stonans, T Trommer, P Hortschansky, S Chubinskaya and JA Mollenhauer. (2006). Expression of bioactive bone morphogenetic proteins in the subacromial bursa of patients with chronic degeneration of the rotator cuff. Arthritis Res Ther 8:R92.
26. Rui YF, PPY Lui, YM Wong, Q Tan, and KM Chan. BMP-2 stimulated non-tenogenic differentiation and promoted proteoglycan deposition of tendon-derived stem cells (TDSCs) in vitro. J Orthop Res, accepted.
27. Airas L, J Niemela and S Jalkanen. (2000). CD73 engagement promotes lymphocyte binding to endothelial cells via a lymphocyte function-associated antigen-1-dependent mechanism. J Immunol 165:5411–5417.
28. Ode A, J Kopf, A Kurtz, K Schmidt-Bleek, P Schrade, P Kolar, F Buttgereit, K Lehmann, DW Hutmacher, GN Duda and G Kasper. (2011). CD73 and CD29 concurrently mediate the mechanically induced decrease of migratory capacity of mesenchymal stromal cells. Eur Cell Mater 22:26–42.
29. Andrade CM, PL Lopez, BT Noronha, MR Wink, R Borojevic, R Margis, G Lenz, AM Battastini and FC Guma. (2011). Ecto-5′-nucleotidase/CD73 knockdown increases cell migration and mRNA level of collagen I in a hepatic stellate cell line. Cell Tissue Res 344:279–286.
30. Rallapalli S, DK Bishi, RS Verma, KM Cherian and S Guhathakurta. (2009). A multiplex PCR technique to characterize human bone marrow derived mesenchymal stem cells. Biotechnol Lett 31:1843–1850.
31. Ponta H, L Sherman and PA Herrlich. (2003). CD44: from adhesion molecules to signaling regulators. Nat Rev Mol Cell Biol 4:33–45.
32. Zhu H, N Mitsuhashi, A Klein, LW Barsky, K Weinberg, ML Barr, A Demetriou and GD Wu. (2006). The role of the hyaluronan receptor CD44 in mesenchymal stem cell migration in the extracellular matrix. Stem Cells 24: 928–935.
33. Pham PV, NL Phan, NT Nguyen, NH Truong, TT Duong, DV Le, KD Truong and NK Phan. (2011). Differentiation of breast cancer stem cells by knockdown of CD44: promising differentiation therapy. J Transl Med 9:209.

Address correspondence to:
Prof. Pauline Po Yee Lui
Department of Orthopaedics and Traumatology
Faculty of Medicine
The Chinese University of Hong Kong
Rm. 74025, 5/F
Clinical Sciences Building
Shatin
Hong Kong SAR
China

E-mail: pauline@ort.cuhk.edu.hk

Received for publication October 6, 2012
Accepted after revision October 29, 2012
Prepublished on Liebert Instant Online October 29, 2012